Geology

Zonally symmetric changes in the strength and position of the Southern Westerlies drove atmospheric CO_2 variations over the past 14 k.y.

M.-S. Fletcher and P.I. Moreno

Geology published online 29 March 2011;
doi: 10.1130/G31807.1

Geology, published online on 29 March 2011 as doi:10.1130/G31807.1

Zonally symmetric changes in the strength and position of the Southern Westerlies drove atmospheric CO_2 variations over the past 14 k.y.

M.-S. Fletcher[1], and P.I. Moreno[1,2]
[1]Institute of Ecology and Biodiversity, University of Chile, Santiago, Las Palmeras 3425, Ñuñoa, Chile
[2]Department of Ecological Sciences, University of Chile, Santiago, Las Palmeras 3425, Ñuñoa, Chile

ABSTRACT

Terrestrial records from 41 to 52°S across the Southern Hemisphere reveal nearly synchronous multimillennial trends in moisture derived from the Southern Westerly Winds (SWW) since 14 ka, pointing to a marked zonal symmetry in SWW changes across a broad swath of the southern middle latitudes. The data suggest a southward shift of the SWW that coincided with a rapid atmospheric CO_2 rise starting ca. 12.5 ka, a widespread decline in SWW strength between ca. 10 and 7 ka contemporaneous with an ~8 ppm reversal in the deglacial atmospheric CO_2 rise, followed by stronger SWW and a steady multimillennial increase in CO_2 until the preindustrial maximum. We conclude that zonally symmetric changes in the intensity of the SWW at multimillennial time scales have covaried with atmospheric CO_2 variations since 14 ka, and suggest that changes in the SWW–Southern Ocean coupled system have influenced the atmospheric CO_2 concentration through wind-driven upwelling of CO_2-rich deep waters in the high southern latitudes.

INTRODUCTION

The Southern Westerlies (Southern Westerly Winds, SWW) are a zonally symmetric component of the global atmospheric system that dictate the climate of regions between 30°S and 60°S, drive Southern Ocean and deep-water circulation, and have recently been recognized as a key factor in global atmospheric CO_2 variations (Toggweiler et al., 2006; Anderson et al., 2009). Driven primarily by equator to pole thermal and atmospheric pressure gradients, the SWW have changed in intensity and latitudinal position over the recent and deep past (e.g., Shulmeister et al., 2004; Toggweiler, 2009). Most regional syntheses of paleoclimate data relevant for deciphering past SWW behavior, conceptual and numerical paleoclimate models, however, have not examined the behavior of the SWW along a time continuum since the Last Glacial Maximum (LGM) and across their entire range of influence in the Southern Hemisphere landmasses.

Recent studies that apply general circulation model (GCM) simulations conducted under the Paleoclimate Modeling and Intercomparison Project Phase II (PMIP2) have examined changes in the SWW during two contrasting time slices: the LGM (21 ka) and the middle Holocene (6 ka) (Rojas et al., 2009; Rojas and Moreno, 2011). Important divergences in SWW behavior among models in the preindustrial and paleosimulations run under the same boundary conditions highlight the limitations of current models and the complexity of modeling southern middle- and high-latitude climate. Taken at face value, the simulations suggest weaker and less symmetric SWW during the LGM with a marginal northward shift in the southeastern Pacific sector (Rojas et al., 2009), in contrast to a zonally symmetric and slight northward shift (1°–3°) during the 6 ka simulations (Rojas and Moreno, 2011). If correct, these results point to a fundamental difference in the mode of SWW response to the end members of climate variability during the last glacial-interglacial cycle, with zonal symmetry dominating the middle Holocene simulation. Recent studies have linked atmospheric CO_2 variations to changes in the position and strength of the SWW through their influence on biological and physical processes in the Southern Ocean (Toggweiler et al., 2006) during the LGM (Anderson et al., 2009), the Last Glacial Termination (Anderson et al., 2009; Denton et al., 2010) and the Holocene (Moreno et al., 2010). However, most inferences on past latitudinal shifts of the SWW are based on paleoclimate data relevant for monitoring their influence in areas located north of the region of maximum winds speeds (~50°S) (e.g., Lamy et al., 2001; Jenny et al., 2003). One shortcoming of this approach is the inability to distinguish SWW latitudinal displacements from intensity variations.

The relative abundance of radiocarbon-dated records spanning the past 14 k.y. in Southern Hemisphere landmasses affected by the SWW allows reconstructing spatiotemporal variations in the SWW influence, a necessary step for testing GCM outputs and mechanisms of atmospheric CO_2 variations. Here we synthesize and analyze terrestrial paleoenvironmental records from 41 to 52°S in Australia, New Zealand, and southern South America (Fig. 1) to identify multimillennial trends in SWW activity since 14 ka in an effort to elucidate whether symmetrical and synchronous changes in the SWW have dominated the Holocene, and to determine whether this structure of changes is consistent with ideas stressing the role of the SWW as a primary driver of natural atmospheric CO_2 variation during the present interglacial. The similar ecology, climate, and geography of middle- to high-latitude Southern Hemisphere landmasses offer a unique opportunity to synthesize paleoenvironmental data from within the SWW zone of influence. In particular, Southern Hemisphere landmasses between 41°S and 52°S share remarkable affinities, including north-south mountain ranges that intercept the SWW and induce a strong orographic effect that results in a hyperhumid west and sub-humid to semi-arid east; *Nothofagus* and Podocarpaceae dominant rainforest vegetation; and zonally symmetric correlations between SWW strength and precipitation (Fig. 2).

Trans–South Pacific Changes in Moisture Balance

Changes in the position and strength of the SWW significantly influence moisture regimes in the middle- to high-latitude Southern Hemisphere landmasses. Poleward displacement of the SWW results in weaker westerly flow over Southern Hemisphere landmasses north of its modern core (~50°S); equatorward displacement results in stronger flow. Weaker westerly flow decreases precipitation in western regions; stronger

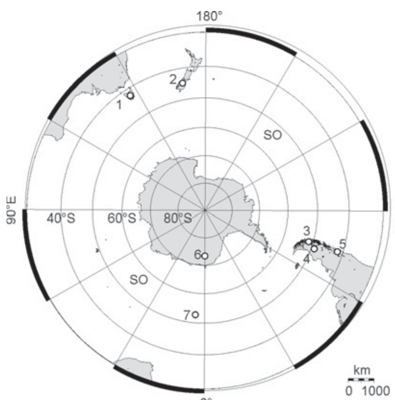

Figure 1. Map showing sites discussed in text. SO—Southern Ocean; 1—Tasmania; 2—South Island, New Zealand; 3—Lago Guanaco; 4—Lago Cardiel; 5—Lago Condorito; 6—EPICA (European Project for Ice Coring in Antarctica) Dome C; 7—Southern Ocean core TN057–13PC.

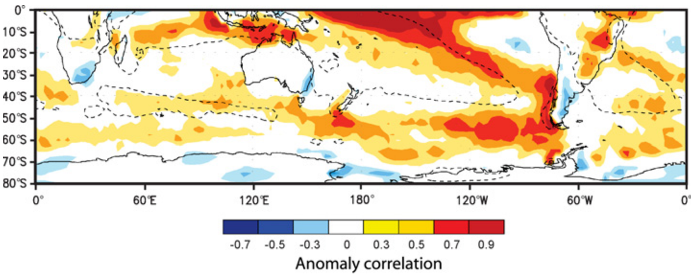

Figure 2. Map showing correlation between monthly anomalies of precipitation and 850 hPa zonal wind strength from equator to 80°S. Dashed lines outline regions where annual mean precipitation exceeds 1000 mm yr^{-1} (Garreaud, 2007).

westerly flow increases precipitation. In eastern regions, weaker westerly flow permits incursions of easterly sourced precipitation from the oceans to the east and lessens the evaporative potential of foehn winds, resulting in wetter conditions; stronger westerly flow inhibits these incursions and intensifies the evaporative potential of foehn winds, resulting in drier conditions (McGlone et al., 1993; Garreaud, 2007; Hendon et al., 2007). This relationship between moisture balance and SWW strength is important in a paleoclimate context, as it implies that reconstructions of moisture balance from within the SWW zone of influence may indirectly proxy relative SWW wind strength. Using these simple relationships we examine published paleoclimate records to decipher past changes in SWW influence since 14 ka across the mid-latitude Pacific landmasses.

Southern South America

Two pollen records from west of the Patagonian Andes, Lago Condorito (LC; 41°S) and Lago Guanaco (LG; 52°S), both located in regions where precipitation is positively correlated with SWW wind speed (Fig. 2), straddle the modern SWW core and display synchronous and covariable multimillennial trends in moisture balance (Moreno et al., 2010). These variations are captured by paleovegetation indices (PI) calculated for each site (LC-PI, Fig. 3A; LG-PI, Fig. 3I; Moreno et al., 2010; see the GSA Data Repository[1]) that reveal above average (LC-PI) or rising (LG-PI) moisture levels between 14 and 11 ka, and 6.8 and 2 ka, and levels below the mean between 11 and 6.8 ka. Trends in moisture diverge after 5 ka, with the LC-PI displaying a multimillennial decrease in moisture at the northern edge of the SWW and the LG-PI displaying a multimillennial increase south of the modern SWW core. Positive anomalies in fire activity are evident in stratigraphic records located in southern Chile and Argentina (30–55°S) between 12.5 and 11.5 ka, and 11 and 7.5 ka, coincident with a decline in precipitation during the late-glacial humid phase in northwestern Patagonia (LC-PI), and the multimillennial dry phase in western Patagonia during the early Holocene (Whitlock et al., 2007; Moreno et al., 2010), respectively. Negative anomalies in fire activity prevailed between 7 and 3 ka, coeval with a multimillennial trend toward high-moisture patterns in western Patagonia.

Lago Cardiel is a large closed-basin lake located east of the Andes in central Patagonia (49°S), a region where modern precipitation is negatively correlated with SWW wind speed (Fig. 2). The lake level of Lago Cardiel shows a dramatic increase starting at 12.5 ka and reaching levels above modern between 11 and 8 ka (Fig. 3B), a timing nearly identical to the southern South America positive anomalies in fire occurrence and low relative moisture in western Patagonia (Fig. 3). These data reveal clear antiphasing of moisture regimes east and west of the Andes that

[1]GSA Data Repository item 2011139, methods and chronology, is available online at www.geosociety.org/pubs/ft2011.htm, or on request from editing@geosociety.org or Documents Secretary, GSA, P.O. Box 9140, Boulder, CO 80301, USA.

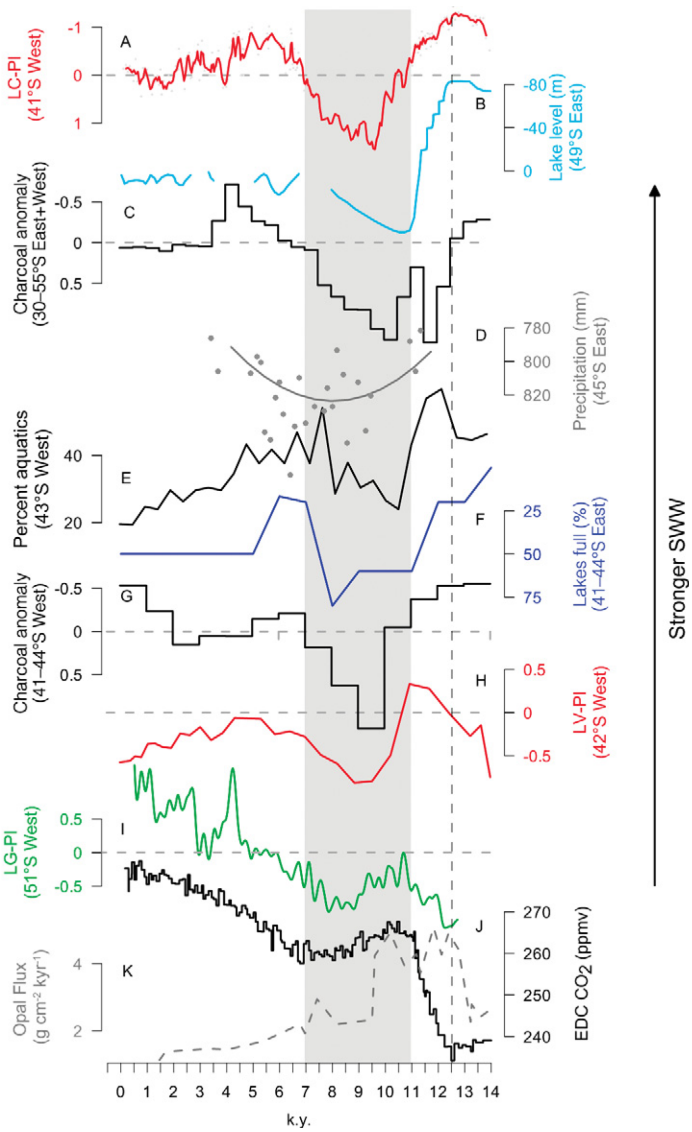

Figure 3. A: Lago Condorito paleovegetation index (LC-PI). Positive values indicate lower relative moisture; negative values indicate higher relative moisture (Site 6, Fig. 1; Moreno et al., 2010). B: Lago Cardiel lake level (Site 4, Fig. 1; Ariztegui et al., 2009). C: Southern South America charcoal anomalies (Power et al., 2008). D: Otago precipitation (Site 2, Fig. 1; Prebble and Shulmeister, 2002). E: Okarito Bog aquatic pollen (Site 2, Fig. 1; Newnham et al., 2007). F: Eastern and central Tasmanian lake levels (Site 1, Fig. 1; Harrison and Dodson, 1993). G: Western Tasmanian charcoal anomalies; steps represent 1 k.y. time slices (Site 1, Fig. 1; Fletcher and Thomas, 2010) (see the Data Repository [see footnote 1]). H: Lake Vera paleovegetation index (LV-PI). Positive values indicate higher relative moisture; negative values indicate lower relative moisture (Site 1, Fig. 1; see the Data Repository). I: Atmospheric CO_2 data from EPICA (European Project for Ice Coring in Antarctica) Dome C (EDC; Site 6, Fig. 1; Monnin et al., 2004). J: Lago Guanaco paleovegetation index (LG-PI). Positive values indicate higher relative moisture; negative values indicate lower relative moisture (Site 3, Fig. 1; Moreno et al., 2010). K: Opal flux for core TN057–13PC (Site 7, Fig. 1; Anderson et al., 2009). For chronological information, see the Data Repository. Horizontal dashed lines represent mean values of records standardized to entire record mean. Vertical dashed line indicates commencement of southward shift of southern westerly winds (SWW) ca. 12.5 ka as inferred from sites located north of SWW core (~50°S). Latitude and location east or west of orographic divide are indicated for each proxy.

mirrors the relationship between precipitation and SWW wind speed in the modern climate (Fig. 2), suggesting that the transgressive lake phase in Lago Cardiel can be attributed to precipitation sources other than the SWW. Furthermore, the onset of the large-magnitude lake level rise in Lago Cardiel is synchronous with a precipitation decline in northwestern Patagonia, a positive anomaly in fire activity, and increasing precipitation in southwestern Patagonia, suggesting a southward shift of the SWW between 12.5 and 11.5 ka.

New Zealand

Aquatic pollen content in the Okarito Bog pollen record (Newnham et al., 2007) from the west coast of South Island, New Zealand (43°S; Fig. 1), located in a high-rainfall west coast region where precipitation is positively correlated with SWW wind speed (Fig. 2), shows clear multimillennial trends that relate to local hydrological balance (Fig. 3E), i.e., high abundance between 14 and 11 ka, a significant reduction between 11 and 8 ka, a rise between 8 and 5 ka, and a multimillennial decline to the present. Prebble and Shulmeister (2002) published a phytolyth-based quantitative reconstruction of effective precipitation in Otago, New Zealand (45°S; Fig. 1), a region where precipitation is negatively correlated with SWW wind speed in the modern climate (McGlone et al., 1993), revealing an increase in effective precipitation beginning at 12 ka, peaking ca. 8.5 ka, and decreasing toward 4 ka (Fig. 3D). A clear antiphasing of moisture balance changes is apparent over New Zealand between ca. 12 and 4 ka, and mirrors the relationship between SWW flow and precipitation in the modern climate. The multimillennial pattern features a period of enhanced SWW influence over New Zealand between 14 and 11 ka, and 8 and 5 ka, and an attenuation between 11 and 8 ka.

Tasmania

A pollen record from Lake Vera in western Tasmania, Australia (42°S; Fig. 1) (Macphail, 1979), where local precipitation correlated positively with SWW wind speed (Fig. 2), allows the calculation of a paleovegetation index (LV-PI) that shows distinct moisture driven compositional changes in rainforest vegetation since 14 ka (see the Data Repository). The LV-PI suggests above average moisture between 14 and 11 ka, and 7 and 4.5 ka, and low relative moisture between 11 and 7 ka, and 4.5 and 0 ka (Fig. 3H). The regional charcoal curve for western Tasmania (41–43°S) (Fig. 2G; Fletcher and Thomas, 2010; see the Data Repository) displays high charcoal values between 10 and 7 ka and increasing charcoal between 5 and 2 ka, reflecting increased burning during periods of low relative moisture indicated by the LV-PI. A regional lake-level reconstruction for Tasmania (Fig. 3F), dominated by lakes located east of the central divide (Harrison and Dodson, 1993), areas in which precipitation is negatively correlated to SWW strength (Fig. 2; Hendon et al., 2007), shows a low percentage of lakes full between 14 and 12 ka, and 7 and 5 ka, and a high proportion between 11 and 8 ka, establishing a clear east-west antiphasing of moisture regimes that mirrors the relationship between the SWW and Tasmanian precipitation. We infer a period of enhanced (relative to the 14 k.y. mean) SWW influence over the region between 14 and 11 ka, and 7 and 5 ka, and diminished influence between 11 and 8 ka.

DISCUSSION

Our results reveal zonally symmetric changes in moisture regime over a broad latitudinal band in the southern middle latitudes (41–52°S); a salient feature of this is the clear antiphasing of east-west moisture balances on all landmasses at a multimillennial scale that mirrors the modern relationship between SWW wind speed and precipitation (Fig. 2). This implies that zonal symmetry has been a stationary feature over the past 14 k.y. We observe two prevailing multimillennial SWW modes since 14 ka. (1) Enhanced SWW flow relative to the 14 k.y. mean between ca. 14–11 and ca. 7–5 ka, manifested as high relative moisture (rainfall) in western regions, driving compositional changes in rainforest vegetation and negating the incidence of fire. In the east, strengthened westerly foehn winds increased evaporation and inhibited incursions of easterly sourced precipitation, resulting in low lake levels. (2) Attenuated SWW flow between ca. 11 and 7 ka manifested as lower moisture, increased burning, and rainforest compositional changes in western regions, while a reduction in evaporative loss from weakened foehn winds and the incursion of moisture from easterly moisture sources prevailed in eastern regions, leading to increased lake levels. Millennial-scale changes are superimposed upon these multimillennial-scale patterns, the most salient of which is a decline in precipitation between 12.5 and 11.5 ka in northwestern Patagonia in the context of above-average hydrologic balance, contemporaneous with intense fire activity, the commencement of a major transgressive phase in Lago Cardiel (Figs. 3A–3C), and increasing moisture in southwestern Patagonia. We observe an apparent breakdown in zonal symmetry between northern and southern sites after 5 ka. This pattern of divergence in moisture regimes is consistent with the regional hydrologic impacts of ENSO (El Niño–Southern Oscillation) variability (Garreaud, 2007) and may reflect the onset of permanent ENSO variability after 5 ka recorded in tropical and subtropical sectors (Tudhope et al., 2001; Moy et al., 2002).

While consistent with earlier conceptual models of SWW change (Markgraf et al., 1992; Shulmeister et al., 2004), our synthesis provides for the first time an analysis of continuous time-series data from across a broad swath of the Southern Hemisphere in regions located entirely within the SWW zone of influence. Our results challenge the long-held tenet of increased SWW influence between 14 and 8 ka in southern Australia that is entrenched in the paleoclimate literature. Given the close resemblance between multimillennial-scale moisture regime changes (Fig. 3) and the modern SWW-driven climatology of this region (Fig. 2), the apparent time-transgressive north-south trend in moisture maxima observed over the past 14 k.y. in southeast Australia, rather than reflecting "increasing moist westerly flow" (Donders et al., 2007, p. 1634), may reflect spatially heterogeneous responses to zonally symmetric changes in SWW influence.

The timing and direction of paleohydrologic changes in records located north and south of the SWW core may afford a solution to unraveling past variations in the intensity and latitudinal position of the SWW, an important facet for understanding past changes in the carbon cycle, as suggested by a recent modeling study that found differences in the direction and magnitude of atmospheric CO_2 change under different scenarios (Tschumi et al., 2008). Our results are consistent with those in Moreno et al. (2010), in which symmetrical paleohydrologic changes in areas with precipitation regimes positively correlated with SWW flow in western-southern South America, north and south of the zone of maximum wind speeds, and changes in SWW intensity over the past 14 k.y. were postulated. The correspondence of these changes with atmospheric CO_2 variations (Fig. 3J) was interpreted by Moreno et al. (2010) as evidence in support of the idea that changes in the SWW–Southern Ocean coupled system govern degassing of the deep ocean.

We note a nearly synchronous decline in SWW-derived moisture in northwestern Patagonia, a rapid lake-level rise in Lago Cardiel (central Patagonia), and increase in fire activity commencing ca. 12.5 ka in sectors located north of the modern SWW core (~50°S). Concurrently, a moisture increase occurred in southwestern Patagonia (Fig. 3I) coeval with enhanced SWW-driven ocean upwelling in the Southern Ocean (Fig. 3K). This latitudinal patterning of changes is consistent with a southward shift of the SWW commencing ca. 12.5 ka, coincident with a rapid increase and resumption of the deglacial rising trend in atmospheric CO_2 (Fig. 3J), lending support to the ocean-atmosphere coupling between the SWW and the Southern Ocean discussed herein. We also note that the steady multimillennial increase in atmospheric CO_2 concentration since ca. 8 ka was unaffected by the apparent breakdown in zonal symmetry at the northern edge of the SWW zone of influence after 5 ka. This change coincided with the establishment of permanent ENSO variability in the tropical Pacific (Tudhope et al., 2001; Moy et al., 2002), a factor known to result in zonal and meridional hydrological asymmetry in the middle to high southern latitudes (Garreaud, 2007). One interpretation of this pattern is that the ENSO variability affected the northern edge of the SWW, but did not affect the SWW–Southern Ocean coupled system.

Based on our collation of paleoclimate data, we conclude that the SWW changed in a zonally symmetric manner at multimillennial scales over the past 14 k.y. These results are consistent with the zonal symmetry and slight equatorward shift (1°–3°) of the SWW in the 6 ka PMIP2 simulations (Rojas and Moreno, 2011). Furthermore, our findings are entirely consistent with paleoenvironmental reconstructions from other high-latitude (>50°S) Southern Hemisphere regions (McGlone and Meurk, 2000; Anselmetti et al., 2009; Waldmann et al., 2010) and indicate (1) a southward shift of the SWW ca. 12.5 ka, and (2) the nearly synchronous hemisphere-wide multimillennial-scale changes in SWW strength discussed herein. The correspondence in timing and direction of these findings with atmospheric CO_2 variations (Fig. 3) (Monnin et al., 2004) provides empirical support for a central role of the SWW in the ventilation of CO_2-rich deep waters in the Southern Ocean (Toggweiler et al., 2006; Anderson et al., 2009; Toggweiler, 2009).

ACKNOWLEDGMENTS

Fletcher is funded by the Institute of Ecology and Biodiversity, Chile, and Moreno is funded by Fondecyt 1070991 and Iniciativa Científica Milenio P05–002, contract PFB-23.

REFERENCES CITED

Anderson, R.F., Ali, S., Bratmiller, L.I., Nielsen, S.H.H., Fleisher, M.Q., Anderson, B.E., and Burkle, L.H., 2009, Wind-driven upwelling in the Southern Ocean and the deglacial rise in atmospheric CO_2: Science, v. 323, p. 1443–1448, doi: 10.1126/science.1167441.

Anselmetti, F.S., Ariztegui, D., De Batist, M., Gebhardt, A.C., Haberzettl, T., Niessen, F., Ohlendorf, C., and Zolitschka, B., 2009, Environmental history of southern Patagonia unravelled by the seismic stratigraphy of Laguna Potrok Aike: Sedimentology, v. 56, p. 873–892, doi: 10.1111/j.1365-3091.2008.01002.x.

Ariztegui, D., Gilli, A., Anselmetti, F.S., Goñi, R.A., Belardi, J.B., and Espinosa, S., 2009, Lake-level changes in central Patagonia (Argentina): Crossing environmental thresholds for Late Glacial and Holocene human occupation: Journal of Quaternary Science, v. 25, p. 1049–1192, doi: 10.1002/jqs.1352.

Denton, G.H., Anderson, R.F., Toggweiler, J.R., Edwards, R.L., Schaefer, J.M., and Putnam, A.E., 2010, The last glacial termination: Science, v. 328, 1652, doi: 10.1126/science.1184119.

Donders, T.H., Haberle, S., Hope, G., Wagner, F., and Visscher, H., 2007, Pollen evidence for the transition of the Eastern Australian climate system from the post-glacial to the present-day ENSO mode: Quaternary Science Reviews, v. 26, p. 1621–1637, doi: 10.1016/j.quascirev.2006.11.018.

Fletcher, M.-S., and Thomas, I., 2010, The origin and temporal development of an ancient cultural landscape: Journal of Biogeography, v. 37, p. 2183–2196, doi: 10.1111/j.1365-2699.2010.02363.x.

Garreaud, R.D., 2007, Precipitation and circulation covariability in the extratropics: Journal of Climate, v. 20, p. 4789–4797, doi: 10.1175/JCLI4257.1.

Harrison, S.P., and Dodson, J.R., 1993, Climates of Australia and New Guinea since 18,000 yr B.P., *in* Wright, H.E., Jr., et al., eds., Global climates since the Last Glacial Maximum: Minneapolis, University of Minnesota Press, p. 265–293.

Hendon, H.H., Thompson, D.W.J., and Wheeler, M.C., 2007, Australian rainfall and surface temperature variations associated with the Southern Hemisphere annular mode: Journal of Climate, v. 20, p. 2452–2467, doi: 10.1175/JCLI4134.1.

Jenny, B., Wilhem, D., and Valero-Garces, B.L., 2003, The Southern Westerlies in central Chile: Holocene precipitation estimates based on a water balance model for Laguna Aculeo (33°50′S): Climate Dynamics, v. 20, p. 269–280.

Lamy, F., Hebbeln, D., Röhl, U., and Wefer, G., 2001, Holocene rainfall variability in southern Chile: A marine record of latitudinal shifts of the Southern Westerlies: Earth and Planetary Science Letters, v. 185, p. 369–382, doi: 10.1016/S0012-821X(00)00381-2.

Macphail, M.K., 1979, Vegetation and climates in southern Tasmania since the last glaciation: Quaternary Research, v. 11, p. 306–341, doi: 10.1016/0033-5894(79)90078-4.

Markgraf, V., Dodson, J.R., Kershaw, P.A., McGlone, M.S., and Nicholls, N., 1992, Evolution of late Pleistocene and Holocene climates in the circum-South Pacific land areas: Climate Dynamics, v. 6, p. 193–211, doi: 10.1007/BF00193532.

McGlone, M.S., and Meurk, C.D., 2000, Modern pollen rain, sub-Antarctic Campbell Island, New Zealand: New Zealand Journal of Ecology, v. 24, p. 181–194.

McGlone, M.S., Salinger, M.J., and Moar, N.T., 1993, Paleovegetation studies of New Zealand's climate since the Last Glacial Maximum, *in* Wright, H.E., Jr., et al., eds., Global climates since the last glacial maximum: Minneapolis, Minnesota, University of Minnesota Press, p. 294–317.

Monnin, E., Steig, E.J., Siegenthaler, U., Kawamura, K., Schwander, J., Stauffer, B., Stocker, T.F., Morse, D.L., Barnola, J.M., and Bellier, B., 2004, Evidence for substantial accumulation rate variability in Antarctica during the Holocene, through synchronization of CO_2 in the Taylor Dome, Dome C and DML ice cores: Earth and Planetary Science Letters, v. 224, p. 45–54, doi: 10.1016/j.epsl.2004.05.007.

Moreno, P.I., Francois, J.P., Moy, C.M., and Villa-Martinez, R., 2010, Covariability of the Southern Westerlies and atmospheric CO_2 during the Holocene: Geology, v. 39, p. 727–730, doi: 10.1130/G30962.1.

Moy, C.M., Seltzer, G.O., Rodbell, D.T., and Anderson, D.M., 2002, Variability of El Niño/Southern Oscillation activity at millennial timescales during the Holocene: Nature, v. 420, p. 162–165, doi: 10.1038/nature01194.

Newnham, R.M., Vandergoes, M.J., Hendy, C.H., Lowe, D.J., and Preusser, F., 2007, A terrestrial palynological record for the last two glacial cycles from southwestern New Zealand: Quaternary Science Reviews, v. 26, p. 517–535, doi: 10.1016/j.quascirev.2006.05.005.

Power, M.J., and 82 others, 2008, Changes in fire regimes since the Last Glacial Maximum: An assessment based on a global synthesis and analysis of charcoal data: Climate Dynamics, v. 30, p. 887–907, doi: 10.1007/s00382-007-0334-x.

Prebble, M., and Shulmeister, J., 2002, An analysis of phytolith assemblages for the quantitative reconstruction of late Quaternary environments of the Lower Taieri Plain, Otago, South Island, New Zealand II: Paleoenvironmental reconstruction: Journal of Paleolimnology, v. 27, p. 415–427, doi: 10.1023/A:1020314719427.

Rojas, M., and Moreno, P.I., 2011, Atmospheric circulation changes and neoglacial conditions in the Southern Hemisphere mid-latitudes: Insights from PMIP2 simulations at 6 kyr: Climate Dynamics, doi: 10.1007/s00382-010-0866-3 (in press).

Rojas, M., Moreno, P.I., Kageyama, M., Crucifix, M., Hewitt, C., Abe-Ouchi, A., Ohgaito, R., Brady, E.C., and Hope, P., 2009, The Southern Westerlies during the Last Glacial Maximum in PMIP2 simulations: Climate Dynamics, v. 32, p. 525–548, doi: 10.1007/s00382-008-0421-7.

Shulmeister, J., Goodwin, I., Renwick, J., Harle, K., Armand, L., McGlone, M.S., Cook, E.J., Dodson, J.R., Mayewski, P., and Curran, M., 2004, The Southern Hemisphere westerlies in the Australasian sector over the last glacial cycle: A synthesis: Quaternary International, v. 118–119, p. 23–53, doi: 10.1016/S1040-6182(03)00129-0.

Toggweiler, J.R., 2009, Climate change: Shifting Westerlies: Science, v. 323, 1434, doi: 10.1126/science.1169823.

Toggweiler, J.R., Russell, J.L., and Carson, S.R., 2006, Midlatitude westerlies, atmospheric CO_2, and climate change during the ice ages: Paleoceanography, v. 21, PA2005, doi: 10.1029/2005PA001154.

Tschumi, T., Joos, F., and Parekh, P., 2008, How important are Southern Hemisphere wind changes for low glacial carbon dioxide? A model study: Paleoceanography, v. 23, PA4208, doi: 10.1029/2008PA001592.

Tudhope, A.W., Chilcott, C.P., McCulloch, M.T., Cook, E.R., Chappell, J., Ellam, R.M., Lea, D.W., Lough, J.M., and Shimmield, G.B., 2001, Variability in the El Niño–Southern Oscillation through a glacial-interglacial cycle: Science, v. 291, p. 1511–1517, doi: 10.1126/science.1057969.

Waldmann, N., Ariztegui, D., Anselmetti, F.S., Austin, J.A., Jr., Moy, C.M., Stern, C., Recasens, C., and Dunbar, R.B., 2010, Holocene climatic fluctuations and positioning of the Southern Hemisphere westerlies in Tierra del Fuego (54°S), Patagonia: Journal of Quaternary Science, v. 25, p. 1063–1075, doi: 10.1002/jqs.

Whitlock, C., Moreno, P.I., and Bartlein, P., 2007, Climatic controls of Holocene fire patterns in southern South America: Quaternary Research, v. 68, p. 28–36, doi: 10.1016/j.yqres.2007.01.012.

Manuscript received 5 October 2010
Revised manuscript received 1 December 2010
Manuscript accepted 5 December 2010

Printed in USA